Characterization of a Portable, Light-Weight, Low-Power Chemical Ionization Time-of-Flight Mass Spectrometer

Austin D. Dobrecevich[1,2], Felipe Lopez-Hilfiker[3], Chris J. Wright[2], Urs Rohner[3], Joel A. Thornton[2]

[1]Department of Chemistry, University of Washington, Seattle, 98195, USA
[2]Department of Atmospheric and Climate Science, University of Washington, Seattle, 98195, USA
[3]Tofwerk AG, Thun, 3645, Switzerland

Correspondence to: Joel A. Thornton (joelt@uw.edu)

Abstract.

We have developed and characterized the performance of a portable time of flight chemical ionization mass spectrometer (Portable-TOF-CIMS) capable of detecting trace gases at parts per trillion by volume (*pptv*) mixing ratios in ambient air. The instrument is compact (0.063 m^3), weighs less than 30 kg, and operates on <270 W of 24 VDC power. These characteristics allow it to be readily deployed on a range of mobile or stationary platforms with little electrical or structural engineering considerations. The mass spectrometer achieves a mass resolving power of 1300 ($m/\Delta m$) at mass-to-charge (m/Q) of 381 Th and a mass accuracy of <10 *ppm*. The instrument can operate in both positive or negative polarity and therefore can detect a suite of different analytes depending upon the reagent ion chemistry. We demonstrate the instrument response to inorganic and organic trace gases using iodide anion ($[I]^-$) adduct and benzene cation ($[Bz]^+$) reagent ion chemistries and illustrate its performance sampling ambient air during a multi-week stationary deployment and mobile deployments from two different personal automobiles and from a cargo e-bike using only a battery to power the instrument during operation.

Short Summary

A portable mass spectrometer has been developed to sensitively measure key environmental pollutants at high temporal resolution. Its low power consumption and compact design enable battery-powered operation and deployment in challenging settings such as light aircraft, tall towers, and remote, off-grid locations, providing new insight into atmospheric chemical variability with high spatial and temporal accuracy.

1 Introduction

High time and spatial resolution measurements of air pollutants are fundamental to gaining a greater understanding of the sources and impacts of air pollution, such as on human health (Krilaviciute et al., 2015; Sethi et al., 2013; Tsai, 2016) and on atmospheric and ecosystem processes. Chemical Ionization Mass Spectrometry (CIMS) has become a popular approach to measure an array of gas-phase pollutants *in situ*, both indoors and throughout the atmosphere (Berresheim et al., 2000; Bertram et al., 2011; Huey, 2007; Lee et al., 2014). Chemical ionization coupled to Time-of-Flight mass analyzers (ToF-CIMS), has proven to be well suited for measuring a broad array of ambient organic and inorganic trace gases at high time resolution and signal-to-noise ratio (S/N) with sub parts per trillion by volume (*pptv*) detection limits (Bertram et al., 2011; Hutterli et al., 2022; Kim et al., 2016; Lee et al., 2014; Murschell et al., 2017)**.** However, the size and power needs of such instruments make widespread deployment difficult due to significant infrastructure requirements, including suitable instrument containers, air conditioning, and significant power and specialty compressed gases. These requirements limit the ability to routinely study atmospheric composition, emission sources, and personal exposure at neighbourhood to regional scales (Klepeis et al., 2009; Seigneur et al., 1983; Wallace, 1991; Yeoman et al., 2020), and in remote regions, where the required infrastructure often does not exist.

A lightweight, compact, and low-power ToF-CIMS could enable broader deployability and improve the temporal and spatial resolution of atmospheric composition measurements. With improvements in portability, the variations of short-lived reactive trace gases in different micro-environments and as part of dynamic processes can be explored with higher spatial and temporal resolution, thereby improving source attribution and mechanism elucidation. With the reduced consumption of power and generation of heat, off-the-grid remote location measurements, mobile vehicle measurements in unmodified vehicles, and light aircraft become more feasible without significant engineering or infrastructure demands. Additionally, a small and portable instrument can be positioned very near the sampling source, reducing the need for long inlet lines which are problematic for transmission and quantification of reactive and low volatility compounds (Deming et al., 2019; Li et al., 2023).

Decreasing the size and power demand of a ToF-CIMS can have important implications for performance. Most notably, the length of the mass analyser's drift region, where ion time-of-flight is determined, is traditionally linearly related to the mass resolving power ($m/\Delta m$). Shorter path lengths therefore have a reduced ability to separate isobaric species. While the length of the flight tube has a significant impact on overall size, it contributes marginally to the overall weight and power demand of the instrument. The weight and power consumption of a typical ToF-CIMS instrument is dominated by the vacuum pumps to reach high vacuum, electronics to drive the ion optical elements of the mass analyzer and chamber. These elements are difficult to optimize given the requirement of a differentially pumped interface including multiple RF ion guides, high voltage pulsers and pump power supplies. One way to realize a compact, lightweight and low power instrument is to reduce the gas load of the instrument, particularly in the later stages of the differentially pumped interface. This can be achieved by reducing orifice dimensions in the differentially pumped interface, so that smaller fore pumps and turbo pumps can be used. This reduces power

and weight but also reduces the acceptance area for ions to transit between successive regions of the interface towards the mass analyser. To avoid detrimental loss of sensitivity, the reduction of diameters is compensated by the efficient use of multiple RF devices which can efficiently separate and focus ions into a beam while removing the neutral gas which must be pumped away before ion analysis.

To maintain the benefits of CIMS as a technique (sensitive, fast), a balanced approach must be taken to optimize the weight, power consumption and performance relative to the analytes of interest. This balance is of particular importance for atmospheric studies, where the combined effects of dilution and the chemical transformation of directly emitted compounds into reactive intermediates can result in target analyte concentrations from *ppbv* down to sub *pptv* concentrations. Measurements from moving platforms such as aircraft, ships, or vehicles or stationary high frequency flux approaches place further performance requirements for sensitivity and selectivity at high time resolution.

Here we present a new ToF-CIMS instrument that significantly advances portability while maintaining many of the performance metrics which make CIMS approaches useful for atmospheric studies. The Portable-TOF-CIMS weighs 30 kg requires <270 W of power, and fits within a hand-towable suitcase (Pelican 1610 Protector). The instrument can be operated continuously for ~4 h on a typical (1 kWh) battery weighing (17.9 kg) and the runtime can be easily extended during daytime with consumer grade solar panels when remote operation is required for extended periods of time. The instrument is single person portable and achieves a collision-limited sensitivity of, 30 *ncps/pptv*, limits of detection (LOD, 3σ) of 1.2 *pptv* in 1-minute averages and a mass resolving power (FWHM) of 1300 $m/\Delta m$. We describe the key instrument components and characterize its performance in the laboratory and on a series of small-scale deployments to demonstrate the instruments portability, robustness, and ease of deployment.

2 Experimental

2.1 Portable-TOF-CIMS Instrument Description

The Portable-TOF-CIMS, shown schematically in Fig. 1a and summarized in Table 1, is analogous in overall design to commercially available ToF-CIMS from Tofwerk AG but is much smaller and lighter, with a vacuum system and electronics package capable of supporting either a Vocus AIM ion molecule reaction region (IMR) (Riva et al., 2024), or a PTR reaction region from Tofwerk AG (Yatsyna et al, in prep, Krechmer et al., 2018; Warneke et al., 2011). As such, a summary of the key differences compared to conventional ToF-CIMS instruments is presented here.

One critical point of optimization is the instrument vacuum system. The instrument is pumped by two diaphragm pumps (MD 1, VACUUBRAND) to hold the reaction pressure of the AIM reactor at 100 mbar, under otherwise typical flow conditions of 1800 standard cubic centimetres per minute (SCCM) of ambient air mixed with of reagent ion laden flow drawn through the

IMR region. The reagent ion is generated and provided by passing a flow of up to 250 SCCM of Ultra-High Purity (UHP) Nitrogen (N_2) through a heated permeation tube filled with a reagent ion precursor solution (in this work, benzene with trace methyl iodide (<0.5%)), into a region illuminated by a vacuum ultra-violet lamp (VUV). VUV photoionization generates a high intensity reagent ion population (here, as an example either benzene cations, [Bz]+, or iodide anions, $[I]^-$). The flow from the reagent ion source is immediately mixed with the ambient air sample to produce analyte ions by different chemical ionization mechanisms (Riva et al., 2024).

After ~30 milliseconds of reaction time, determined by the pressure and mass flow through the IMR, the reacted analyte-reagent ion mixture is subsampled through a critical orifice (0.3 mm) into the first stage of a 4-stage vacuum chamber with all pressure stages evacuated using a single split-flow turbomolecular pump (Pfeiffer SF80). In the first stage, held at constant pressure by the drag stage of the turbo pump, ions are focused by a small RF-only quadrupole ion guide and pushed in the axial direction primarily by the expanding gas flow and a weak DC electric field. The focused ion beam passes through another critical orifice into the second stage, held at 1e-2 mbar, where a longer RF-only quadrupole further cools and focuses the ion beam, after which it passes through a lens stack and finally into the ion extraction region of the TOF analyser. Ions are pulsed at 33-50 kHz, *m/Q* 6 - 800 through the Time-of-Flight (TOF) region, where ions fly a V-shaped trajectory to the multi-channel plate (MCP) detectors. The arrival time and intensity are then related to the ion mass-to-charge (*m/Q*) and abundance through a preamplifier and digitizer (SP Devices ADQ14-2C).

The instrument samples and ionizes ambient air continuously and records and displays mass spectra in real-time at a typical rate of 1-10 Hz. For the analysis and evaluation of the instrument presented here, we used $[Bz]^+$ to detect VOCs and ammonia (NH_3) through charge transfer and adduct formation (Aggarwal et al., 2025; Kim et al., 2016), and $[I]^-$ adduct ionization for oxygenated volatile organic compounds (oVOCs), inorganic and organic acids, and reactive halogens, among other species. Both reagent ion chemistries generally produce mass spectra with limited fragmentation and thus lower data complexity which allows many compounds to be quantified accurately even with relatively low mass resolving power. As an example, the detection of gas phase acids, like nitric acid, formic acid, nitrous acid, lactic acid and other mixed organics do not benefit from higher resolution analysers as the ion chemistry provides enough separation by its inherent selectivity. Similarly, there are few interfering isobars for the detection of typical hydrocarbons like toluene, xylene, trimethylbenzene, isoprene, terpenes, and sesquiterpenes with $[Bz]^+$. For many components of reactive nitrogen, reactive halogens or semi-volatile compounds which pose significant sampling challenges when using long inlets, the enhanced portability can, in many cases, eliminate the need for long sample inlets and thereby provide more accurate measurements by removing uncertainties and corrections associated with wall conversion and losses.

The instrument operates in either negative or positive ion mode which can be switched programmatically through software. A polarity change takes approximately 1-2 minutes to switch with a 15 second ramp down of voltages, a 30-60 second waiting

period for stray charges to dissipate and 15 seconds to set the voltages to the new polarity. While this polarity switching speed is not fast enough for fast moving platforms, it is fast enough for stationary monitoring measurements or slow-moving platforms (e.g. ships) an example of this fast switching between $[Bz]^+$ and $[Br]^-$ is shown in Fig S1.

The instrument was calibrated primarily using $[Bz]^+$ using a certified calibration gas mixture comprising of 13 VOCs balanced in nitrogen (Apel-Riemer Environmental, Inc.) with a dynamic dilution system using two mass flow controllers (Bronkhorst model: TOF-101 (30 SCCM) and TOF-102 (2000 SCCM) full scale). The calibration gas mixture composition is shown in Table S1 and contains a standard PTR VOC mixture with a series of hydrocarbons and some ketones. We chose to calibrate to a series of hydrocarbons because they are much easier to quantitatively work with compared to reactive or low volatility compounds which have been demonstrated to react at the collision limit with iodide adducts.

We assume the ion-molecule collision limited sensitivity measured in positive ion mode on the same instrument transfers well within experimental uncertainty to other ion chemistries operated at the same reactor conditions but in negative ion mode as shown previously (Aggarwal et al., 2025). In particular, when ions of positive and negative polarity are generated by the same ion source, the only difference between two reagent ions is the absolute voltage settings, which could impact absolute ion transmission, but all other parameters are explicitly constant (pressures, flows, RF amplitudes, temperature, ion injection into the sample flow). Therefore, the collision limited sensitivity normalized to the measured reagent ion intensities is expected to be similar between the two ion modes, assuming that the differences in collision-limited rate constants between ions and molecules are similar between different reagent ions. This assumption therefore provides a means to determine and compare sensitivities between differently configured instruments by selecting compounds which are not prone to larger calibration uncertainty like lower volatility and in situ synthesized calibrants.

2.2 Portable-TOF-CIMS e-Bike Deployment

As an example of the enhanced portability of the Portable-TOF-CIMS, we deployed the instrument on an unmodified cargo e-Bike (Figure 1b), with a child carrying basket in the front that could accommodate the instrument as well as a small cylinder of UHP N2 (5.0 UHP Nitrogen, Carbagas). A small inlet sample pump (KNF KNDC 850) drew air at ~10 standard liters per minute (slpm) down a ½" PFA sample line 10 cm long. The output of the sample pump was passed through a pressure relief valve before passing through a 20 cm long 4 cm diameter activated carbon trap to generate zero air. This zero air can be delivered via a three-way solenoid valve to programmatically overflow the inlet, at the operator's discretion (5 times during the short ride presented here), which provided a consumable-free instrument zero measurement and reduced nitrogen consumption. The instrument was powered by a Jackery Explorer 1000 battery pack (Model Number: JE-1000D), which on a single charge can run the instrument for ~4 hours of measurement time, and up to 10 hours in full sun with two 200 W solar panels. On the handlebars of the bike a sonic anemometer and GPS unit (Maximet GMX500) recorded the 2D windspeed and direction as well as location data on the same time base as the mass spectra and was integrated into the TOF data files.

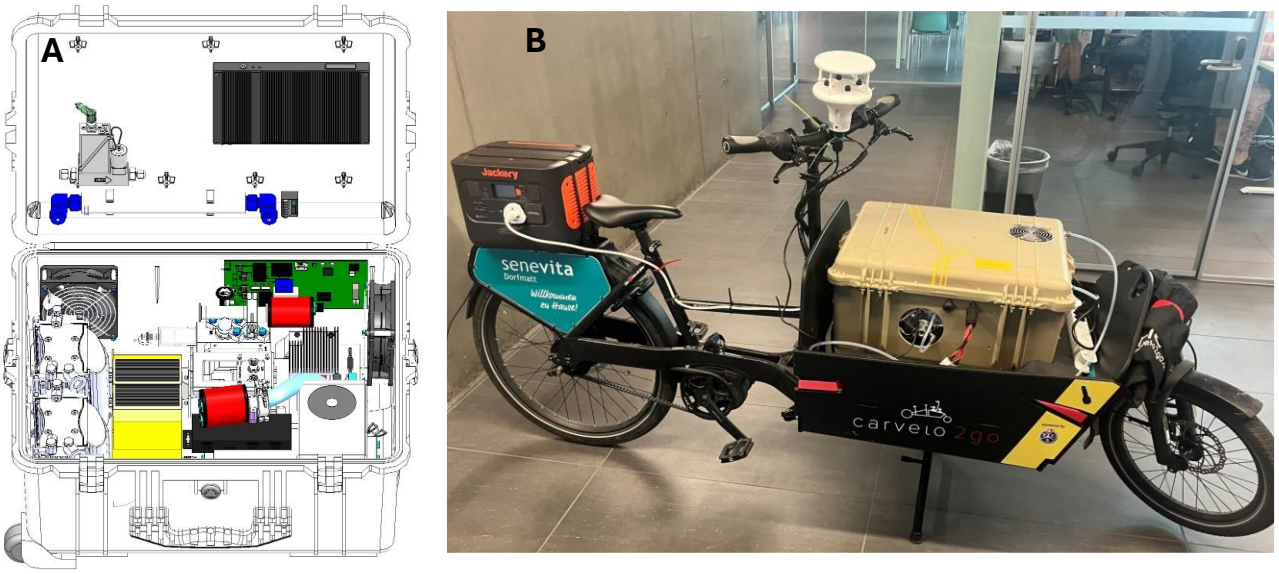

Figure 1: (a) Model Rendering of the Portable-TOF-CIMS, (b) Portable-TOF-CIMS in standalone operation on a battery pack ready for deployment with cargo e-Bike.

Table 1. Instrument technical and performance characteristics. Normalized ion counts were calculated by dividing all masses at each point by the reagent ion signal, then multiplying by 1 million.

Characteristic	Information
Power Consumption	24 VDC, 270 W
Mass	<30 kg
Ion-Molecule-Reaction Region	Vocus AIM (Flow Tube CIMS)
TOF Size	25 cm ToF Region
Mass Resolution ($m/\Delta m$)	~1000-1300
Normalized Sensitivity (Collision limited)	30 ncps/*pptv*
Absolute Sensitivity (Collision limited)	15 cps/*pptv*
$[Bz]^+$ LOD (α-pinene, 1 min, 3σ)	1.2 *pptv*
$[I]^-$ LOD (formic acid, 1 min, 3σ)	5.0 *pptv*

2.4 Data Processing

All data was processed using *Tofware* (v. 4.0) in Igor Pro 9 to calibrate the mass axis with a typical mass accuracy of < *10 ppm* primarily limited by the mass spectral sample frequency (*1 GS/s*). Mass spectral peaks were fit using a three-parameter mass calibration function and Tofware workflows. For $[Bz]^+$ mode, the mass spectrum was calibrated using the signal at the

benzene cation $[C_6H_6]^+$ (78.047 Th), benzene water cluster cation $[C_6H_6H_2O]^+$ (96.058 Th), and the benzene-benzene cluster cation $[C_{12}H_{12}]^+$ (156.094 Th). For $[I]^-$ mode, the mass spectrum was calibrated using the iodide anion $[I]^-$(126.904 Th), iodide clustered to water $[IH_2O]^-$ (144.915 Th), and three-iodide cluster $[I_3]^-$ (380.713 Th). To account for any variations in reagent ion intensity, the recorded signals at each *m/Q* were divided by the instantaneous reagent ion signal and then multiplied by a reference value of one million, yielding units of normalized counts per second per million reagent ion counts. The resulting timeseries data, as well as mass spectra were exported from Tofware and plotted with MATLAB R2022b (The Mathworks, Inc.).

3 Results and Discussion

Compared to a similarly sensitive commercial ToF-CIMS, the Portable-TOF-CIMS requires a factor of 4x less power, occupies a factor 16x less space, and weighs a factor of 6x less than a VOCUS 2R instrument. These reductions in size, weight, and power are achieved while maintaining overall analyte sensitivity in a similar range given that the reagent ion production and chemical ionization conditions remain similar. Sufficient ion focusing by the ion optics allows for smaller critical orifices and thus less pumping downstream of the ionization region, such that the total ion transmission is only reduced by a factor of ~5x impacting detection limits by only $\sqrt{5}$, ~2.5x. The lower ion transmission is compensated by a factor of ~3x by the higher ionization pressure (100 mbar) with a corresponding reduction at the upper end of the linear measurement range (~20-50 *ppbv*). The most notable drawback of the size and power reduction is in limited mass resolving power of 1300-1500 FWHM of the mass analyser.

Instrument sensitivity was determined empirically using a synthetic gas mixture with several analytes of interest, a calibration curve was used to calculate the sensitivity of the instrument to several calibrants including toluene (92.063 Th), m-xylene (106.078 Th), trimethylbenzene (120.094 Th), α-pinene (136.125 Th), and isoprene (106.078 Th) in positive ion mode using $[Bz]^+$ reagent ions as shown in Fig. 2a-b under dry conditions to remove humidity effects from the collision limited sensitivity determination. For normalization, each mass analyte was divided by the detected reagent ion signal, benzene (78.047 Th), throughout the time series and then multiplied by one million. Reagent ion consumption must be managed when operating at elevated ionization pressures, particularly for rather general reagent ions like $[Bz]^+$. We define linear operation ranges where at least 60% of the reagent ion remains compared to the clean air background measurement (shown for our experiments in Fig. S2), as outside of this range, charge competition and secondary effects become more likely impacting the instrument linearity, this relationship is shown in Fig S3. With more selective ions (e.g. $[I]^-$, $[Br]^-$, $[NO_3]^-$, $[SF_6]^-$, $[Cl]^-$) reagent ion titration is less likely but adheres to the same drivers of reagent ion consumption.

Each mixing ratio of calibrants were maintained for ~50 sec before changing to a new concentration. Normalized signal was linearly related to the sampled mixing ratio and constrained to pass through zero as shown in Fig. 2b within the linear response

range for the instrument. In our calibration experiment, by using a multicomponent gas standard we were able to span 0-2.5 *ppbv* of each component simultaneously before depleting reagent ions beyond the defined threshold, corresponding to ~20 *ppbv* of total detected VOC at the collision limited sensitivity. Calibrations were done under dry conditions. The resulting slope demonstrates a reagent ion normalized sensitivity to most hydrocarbons of ±30 ncps/*pptv* ($R^2 = 0.998$), which is similar to the expected collision limited sensitivity for the conditions of the Vocus AIM operated at elevated reactor pressure (Aggarwal et al., 2025; Riva et al., 2024). With these sensitivities we find excellent detection limits of <1 *pptv* (3σ, 1 min avg.) are achieved for much of the mass spectrum, assuming the collision limited sensitivity.

At such high sensitivities the linear range of the instrument is somewhat reduced compared to conventional AIM instruments which operate at 50 mbar. We infer a maximum linear detection range of ~20 *ppbv* under dry conditions, and about 20-50 *ppbv* under ambient humidities due to the general reduction of hydrocarbon sensitives at elevated humidity (Aggarwal et al., 2025; Kim et al., 2016; Puttu et al., 2026). We note that care must be taken when deploying less selective reagent ions at high pressures in highly polluted environments or near heavily emitting point sources. As is the case with any CIMS instrument, deploying highly sensitive ionization schemes in regions with abundant target analytes would require different operation conditions than presented here to maintain linearity, such as reducing sensitivity by reducing pressure, dilution of the ambient air before ionization, or use of a different more selective reagent ion. The instrument as configured and operated here at a reaction pressure of 100 mbar is better suited for pristine environments, where most analytes are within the mid to low *pptv* range (Riva et al., 2024).

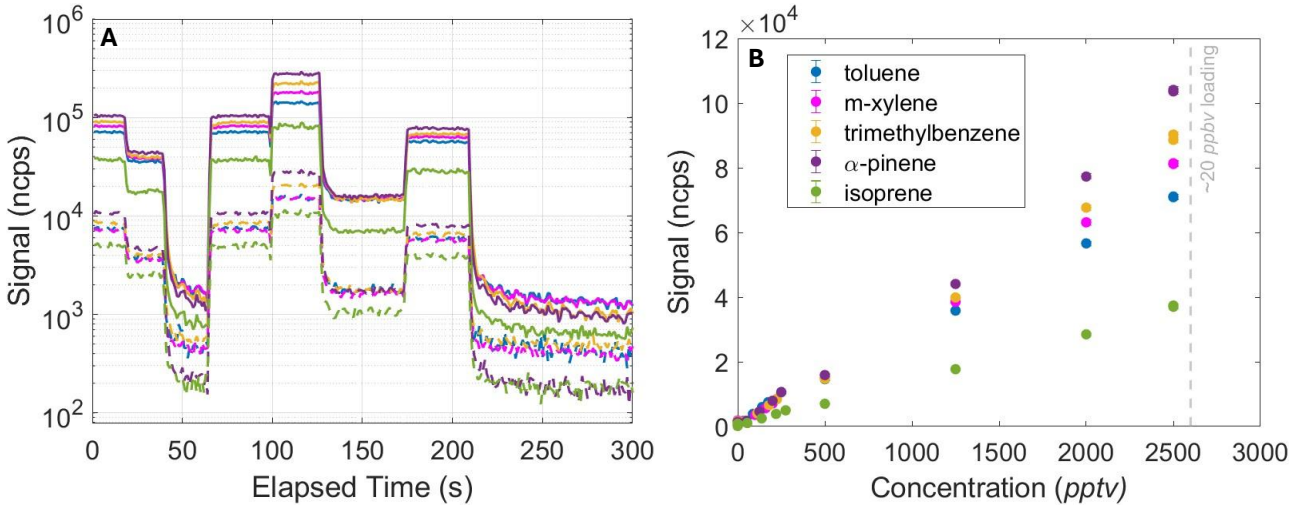

Figure 2: (a) Calibration sequence using a custom calibration gas mixture in $[Bz]^+$ ionization mode, C13 isotopes traced with dashed lines, normalized by reagent ion signal and multiplied by 1e6, (b) Calibration curve for toluene, m-xylene, trimethylbenzene, α-pinene, and isoprene adduct in $[Bz]^+$ ionization mode calculated from time averages in 2a at concentrations that are within the linear response range (retainment of 60% of reagent ion signal).

In Fig. 3a,b we illustrate selective ionization of a potential suite of analytes using $[Bz]^+$ and $[I]^-$ reagent ion chemistries demonstrating that the ionization strategy must be tailored to meet the needs of the user. Each reagent ion chemistry achieves a relatively low background signal across the target range from 50 to 270 Th which ultimately determines detection limits using either ionization strategy. The mass resolving power ($m/\Delta m$) for the instrument in $[I]^-$ reagent ion mode ~1300 shown in Fig. 3c and is representative for positive ion mode as well. A suite of different reagent ion chemistries are possible, such as ammonium cations, acetone cations, protonated ethanol, bromide anions, acetate anions, and nitrate anions with adjustments to the reagent ion precursors and ion guide voltages before detection with the mass analyser.

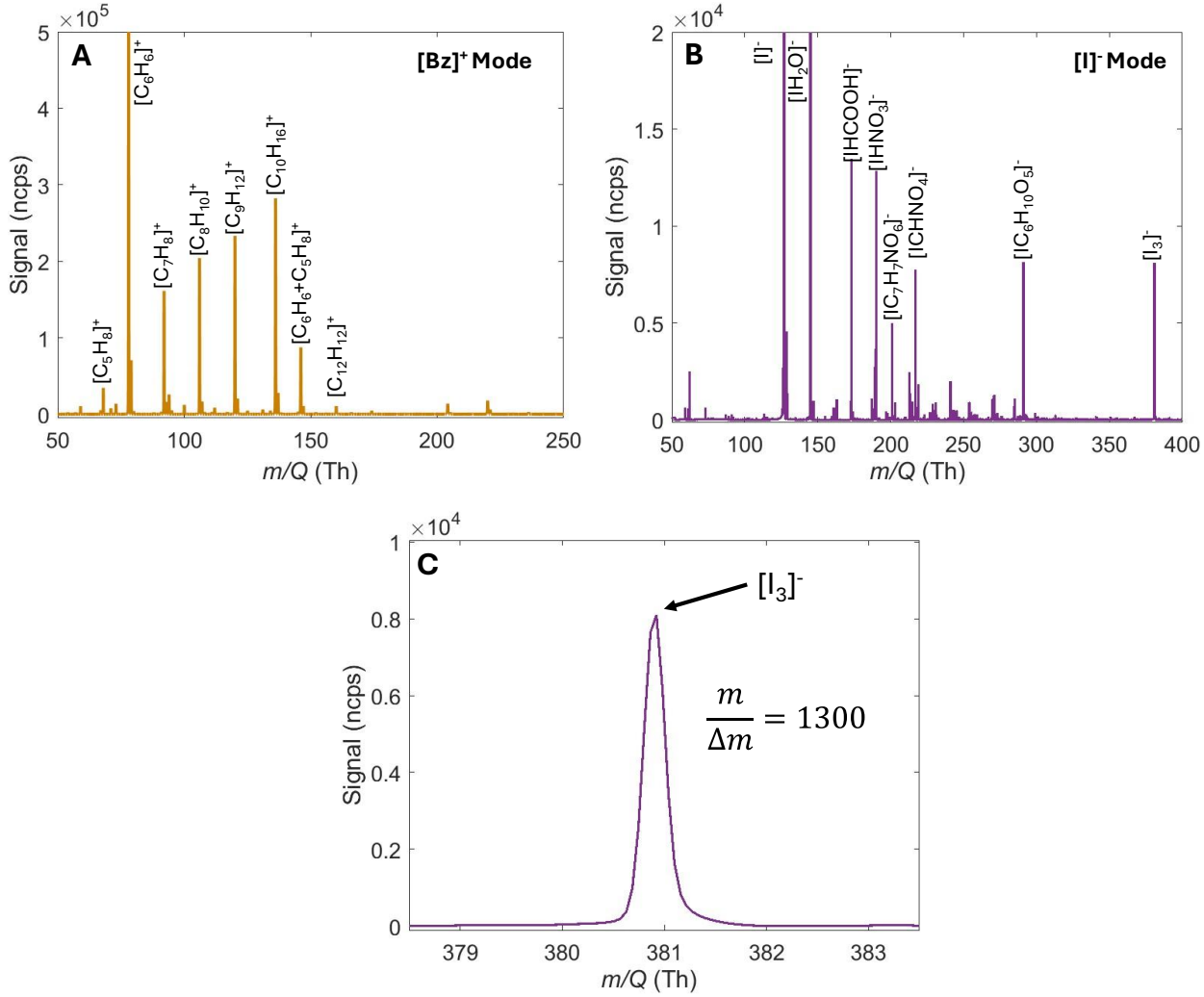

230 **Figure 3: (a) Normalized high-resolution mass spectrum of a calibration gas over lab air in $[Bz]^+$ mode with labelled analyte signals. (b) Normalized high-resolution mass spectrum of air measurements in the field in iodide anion mode with labelled analyte signals. (c) Zoom in on I_3^- cluster signal illustrating representative peak widths for the high-resolution mass spectrum in Fig. 3b.**

In Fig. 4, we show that with a resolving power of ~1300, and assuming a collision-limited sensitivity of 30 normalized ion counts per *pptv*, the Portable-TOF-CIMS using $[Bz]^+$ and $[I]^-$ reagent ions achieves 3σ-LOD in the range of 0.075 to 1.5 *pptv* 235 for much of the mass spectrum with some individual detection limits higher due to the presence of persistent backgrounds present from reagent ion impurities, zero gas impurities. In general, at *m/Q* less than 100, the measurement is often background limited (i.e, even the cleanest air has detectable contaminants in the *pptv* range) while at higher masses (*m/Q* >200) the detection limits become sensitivity limited (chemical background is negligible). At lower *m/Q*, improvements in sensitivity

result in limited improvement of detection limits, but at higher *m/Q* increases in sensitivity can more directly result in improved ion peak discoverability from the background (S/N)

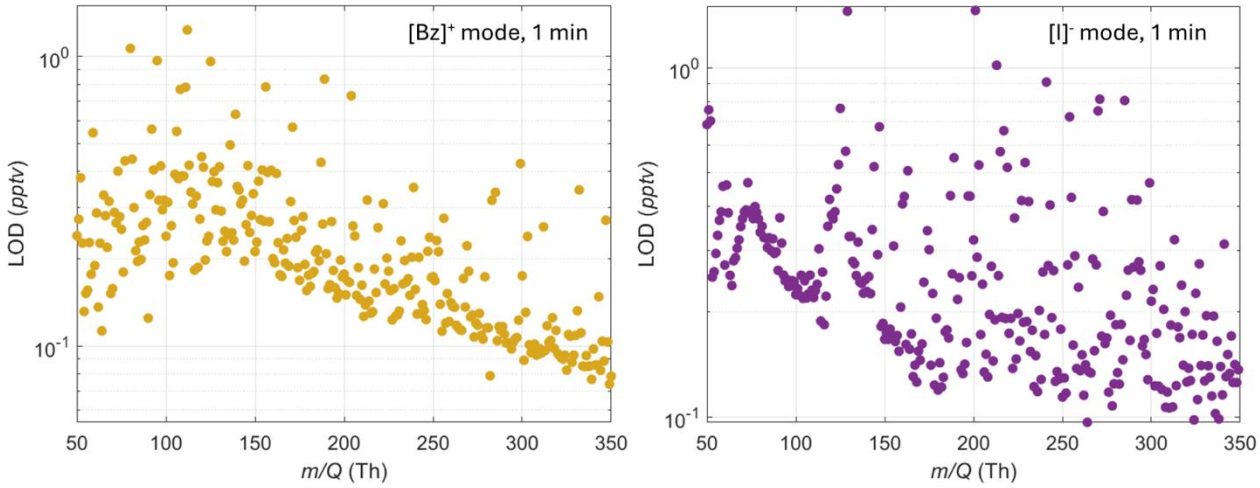

Figure 4: Limits of detection (3σ) for chemical ionization using $[Bz]^+$ and $[I]^-$ reagent ions across the mass spectrum assuming ionization is collision limited and a standard sensitivity in one minute of 30 ncps/*pptv*.

The instrument was operated continuously for 10 days in December using $[I]^-$ reagent ions and sampling ambient air from the fourth floor of an industrial building in Thun, Switzerland, a small town located in a valley near a lake. Mass spectra were collected in five second averages. In Fig. 5a, we show the normalized ion signal timeseries for the *m/Q* consistent with the iodide reagent ion adducts: $[IHONO]^-$ (173.905 Th), $[IHNO_3]^-$ (189.900 Th), $[IC_2H_4O_2]^-$ (186.926 Th), $[IHCOOH]^-$ (172.910 Th), $[IC_6H_{10}O_5]^-$ (288.967 Th). The nitrous acid adduct signal ($[IHONO]^-$) was determined by subtracting the ^{13}C isotope from the formic acid adduct ($[IHCOOH]^-$), and the analytes containing carbon were verified by assessing the expected isotopic distributions. The dynamic range (<1 *pptv* to > 2.5 *ppbv*), *pptv*-level precision and low detection limits of the instrument are evident. In Fig. 5b, we show the average diurnal cycle of $[IHONO]^-$ signal as measured by the Portable-TOF-CIMS, which is consistent with that expected for HONO being emitted by automobile traffic and ground elements with a fast daytime loss by photolysis (Kleffmann, 2007; Sörgel et al., 2011).

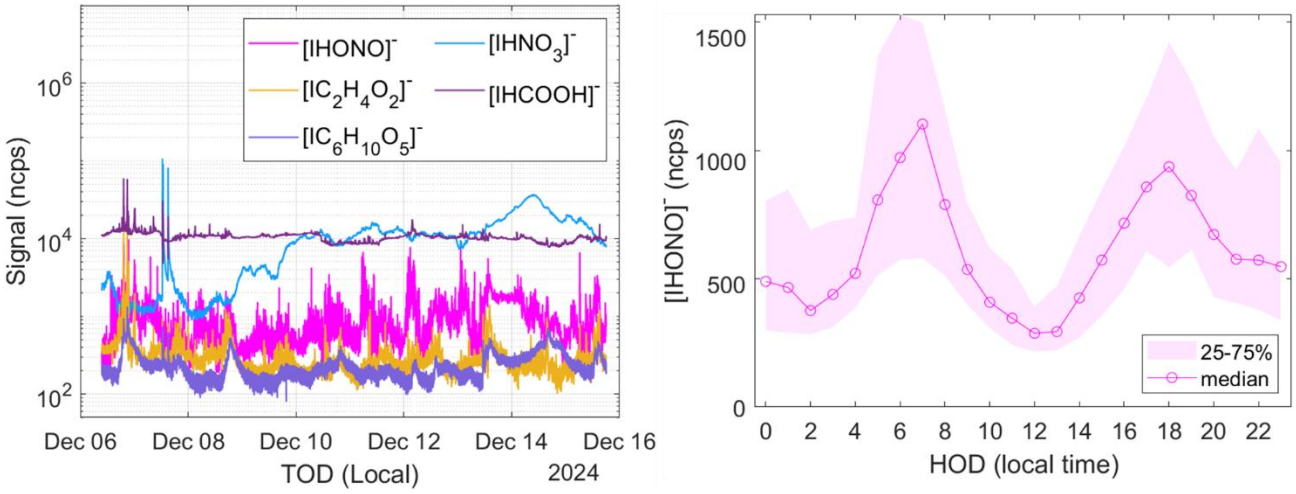

Figure 5: (a) Stationary measurements of key air pollutants for tracing anthropogenic activity with continuous measurements for 10 days using iodide ion chemical ionization. (b) Diurnal cycle using $[IHONO]^-$ Signal averaged hourly. Sensitivities are: 22, 30, 3.4, 8.4 and 30 ncps/*pptv* for $[IHONO]^-$, $[IHNO_3]^-$. $[IC_2H_4O_2]^-$, $[IHCOOH]^-$, $[IC_6H_{10}O_5]^-$, respectively. Further information on sensitivities are shown in Table S2.

The Portable-TOF-CIMS was also deployed in two sampling campaigns using personal automobiles. One campaign was a two-hour drive from Thun to Bern, Switzerland, using the auxiliary battery in a hybrid electric vehicle (Mitsubishi Outlander PHEV) to power the instrument during the drive. The instrument sampled ambient air continuously through an inlet out the passenger window and used $[I]^-$-adduct ionization and the iodide adduct with HONO is plotted in Fig. S4a,b. Measurements are illustrated in supplementary Fig. S4c, showing dynamic mixing ratio changes of various components along congested city streets indicative of fixed and/or mobile point sources of pollution with high temporal and spatial resolution. The instrument was also deployed in Seattle, WA USA, using a personal passenger vehicle (Subaru Outback PZEV) in [Bz]+ mode and a standalone battery pack to power the instrument. As shown in supplementary Fig. S5a-b, significant variations in a woodsmoke tracer (C_7H_8O, consistent with $[Cresol]^+$) detected as a charge transfer product, as well as ammonia, detected as the adduct with [Bz]+, were measured throughout the drive. These results show the different spatial patterns of these two pollution sources: in residential and lower elevation regions the woodsmoke tracer is elevated, while in more commercial and industrial areas, ammonia is relatively elevated.

To further explore the limits of portability and robustness of the instrument, it was placed on an electric cargo bike, as pictured in Fig. 1b, and powered entirely by a battery pack. The bike was then driven around the city of Thun, Switzerland to probe atmospheric composition and pollution sources along a major bike/walk path following the Aare River, as well as along some major thoroughfares for bus, industrial, and personal vehicles including the central bus station located at Thun, Bahnhof. Normalized signals at several *m/Q* are plotted in Fig. 7a-d consistent with the $[I]^-$ adducts with HONO (173.905 Th), HNO_3

(189.900 Th), $C_5H_{10}O_3$ (244.967 Th), and $C_6H_{10}O_5$ (288.967 Th), respectively. The latter two *m/Q* are consistent with that of levoglucosan ($C_6H_{10}O_5$), a known wood smoke tracer commonly detected by I^- adduct ionization, and a likely oxidation product of naphthalene $C_5H_{10}O_3$), such as an oxo-naphthoquinone, which are known to be emitted by diesel exhaust. In areas with heavy traffic, including around the main bus station and along the main roads, HONO, HNO_3, and $C_5H_{10}O_3$ related m/Q exhibited elevated signals, consistent with expectations that these species are derived primarily from anthropogenic pollution. Notably, while both HONO and HNO_3 are related to nitrogen oxide emissions, their spatial distributions were not particularly well correlated. This behaviour is also consistent with expectations as the formation of HNO_3 requires significant atmospheric processing and it has a relatively long lifetime (hours to days), while HONO is mostly directly emitted with a short lifetime (min). Around the train station, indicated by purple arrow in Fig. 7a, HONO mixing ratios were at their highest, indicating an elevated level of fuel combustion emissions in this area (Thun traffic bottleneck, city buses), whereas HNO_3 reached its highest mixing ratios downwind of the urban areas over larger spatial domains. In contrast, in the waterfront city park with only pedestrian paths, mixing ratios of anthropogenic/vehicle pollution tracers (Fig. 7a-c) were relatively low compared to city streets, except for $C_6H_{10}O_5$ (e.g. levoglucosan). Riding through a lakeside city park, a small campfire was active for grilling, indicated by the orange arrow on Figure 7d and the significantly elevated signal at *m/Q* consistent with $C_6H_{10}O_5$ adduct with iodide (e.g. levoglucosan). The instrument operated uninterrupted during the ~4-hour e-Bike deployment demonstrating the stability of the instrument electronics, computer control and sampling system even in a relatively primitive mobile platform.

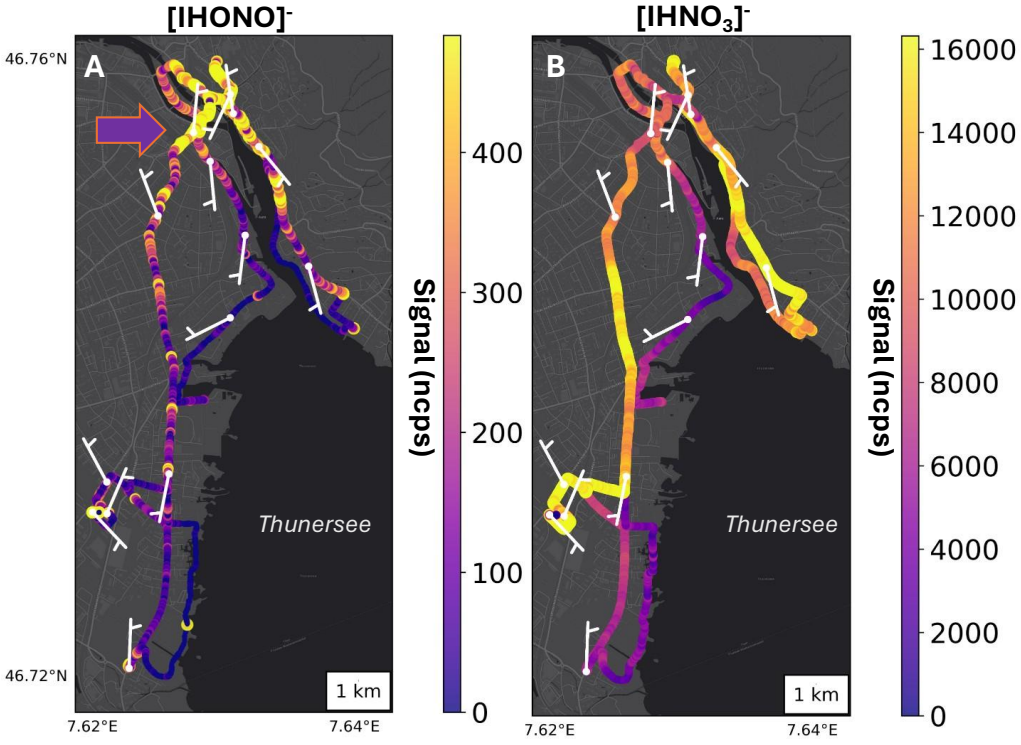

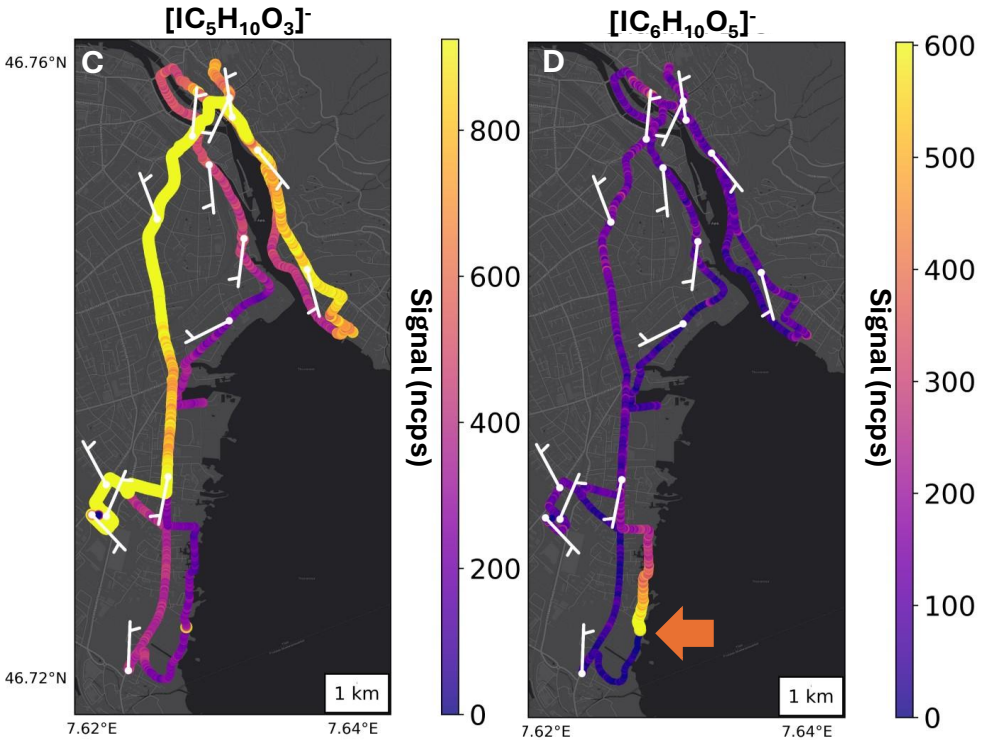

Figure 7: e-Bike Deployment Data of Portable-TOF-CIMS in Iodide ion Mode overlayed with wind barbs and signal profiles of different key pollution species with colormap in units of normalized cps (a) Signal profile of m/Q consistent with iodide ion adduct with nitrous acid (173.905 Th) and purple arrow pointing to major bus station in Thun. (b) Signal profile of m/Q consistent with iodide ion adduct with nitric acid (189.900 Th). (c) Signal profile of m/Q consistent with $C_5H_{10}O_3$ (244.967 Th) adduct with iodide ion. (d) . Signal profile of *m/Q* consistent with $C_6H_{10}O_5$ (288.967 Th) adduct with iodide ion. Estimated sensitivities are: 22, 30, 30, and 30 ncps/*pptv* for $[IHONO]^-$, $[IHNO_3]^-$, $[IC_5H_{10}O_3]^-$, $[IC_6H_{10}O_5]^-$, respectively. Further information on sensitivities are shown in Table S2. Maps powered by ©ESRI Sources: Esri, HERE, Garmin, ©OpenStreetMap contributors, and the GIS user community.

4 Conclusion

The Portable-TOF-CIMS shows promise for enhanced portability for air pollution characterization at the point-source to neighbourhood scale, and for enabling deployment in remote environments lacking access to suitable power or infrastructure. The low power needs and compact size allow for operation of the instrument on battery power, as well as in situations where larger size or weight are not possible such as aboard light aircraft, high instrument towers, and remote off-the-grid locations. The instrument was operated in several different environments and showed high sensitivity and stability on par with larger commercially available CIMS instrumentation. *In-situ* measurements made with the instrument are consistent with expected ambient concentrations and reflect expected chemical phenomena for key analytes. The instrument's relatively low mass

resolving power ultimately restricts its ability to unambiguously assign molecular composition to detected ions, mandating the use of selective reagent ion chemistries with minimal fragmentation, or coupling to a chromatography or ion mobility system, which could negatively affect ease of deployment. Increased efforts for the further miniaturization of the Portable-TOF-CIMS will be advantageous for more widespread and routine measurements of atmospheric or indoor air composition.

Code and Data Availability

All code and data used in the manuscript can be made available upon request.

Author Contribution

ADD: Methodology, Data curation, Formal analysis, Investigation, Software, Validation, Visualization, Writing - original draft, Writing - review & editing.

FLH: Conceptualization, Methodology, Data curation, Formal analysis, Investigation, Validation, Visualization, Writing- review & editing.

CJW: Data Validation, Visualization, Writing- review & editing.

UR: Conceptualization, Methodology, Data curation, Formal analysis, Investigation, Validation, Instrument hardware development, Writing- review & editing,

JAT: Conceptualization, Investigation, Methodology, Funding acquisition, Project administration, Resources, Supervision, Writing - review & editing.

Competing Interests

All authors declare that they have no conflict of interest. Felipe Lopez-Hilfiker and Urs Rohner are employees of Tofwerk AG who is a supplier of chemical ionization time of flight mass spectrometers.

Acknowledgements

The authors thank staff at the University of Washington, in particular Dennis Cannuelle, and Tofwerk AG for their dedication and support of this research.

Funding Sources

This project was funded by the Arnold and Mabel Beckman Foundation.

References

Aggarwal, S., Bansal, P., Wang, Y., Jorga, S., Macgregor, G., Rohner, U., Bannan, T., Salter, M., Zieger, P., Mohr, C., and Lopez-Hilfiker, F.: Identifying key parameters that affect sensitivity of flow tube chemical ionization mass spectrometers, https://doi.org/10.5194/egusphere-2025-696, 6 March 2025.

Berresheim, H., Elste, T., Plass-Dülmer, C., Eiseleb, F. L., and Tannerb, D. J.: Chemical ionization mass spectrometer for long-term measurements of atmospheric OH and H2SO4, Int. J. Mass Spectrom., 202, 91–109, https://doi.org/10.1016/S1387-3806(00)00233-5, 2000.

Bertram, T. H., Kimmel, J. R., Crisp, T. A., Ryder, O. S., Yatavelli, R. L. N., Thornton, J. A., Cubison, M. J., Gonin, M., and Worsnop, D. R.: A field-deployable, chemical ionization time-of-flight mass spectrometer, Atmospheric Meas. Tech., 4, 1471–1479, https://doi.org/10.5194/amt-4-1471-2011, 2011.

Deming, B. L., Pagonis, D., Liu, X., Day, D. A., Talukdar, R., Krechmer, J. E., De Gouw, J. A., Jimenez, J. L., and Ziemann, P. J.: Measurements of delays of gas-phase compounds in a wide variety of tubing materials due to gas–wall interactions, Atmospheric Meas. Tech., 12, 3453–3461, https://doi.org/10.5194/amt-12-3453-2019, 2019.

Huey, L. G.: Measurement of trace atmospheric species by chemical ionization mass spectrometry: Speciation of reactive nitrogen and future directions, Mass Spectrom. Rev., 26, 166–184, https://doi.org/10.1002/mas.20118, 2007.

Hutterli, M., Pospisilova, V., and Gonin, M.: Time-Of-Flight Mass Spectrometers Made in Switzerland: Examples of Mobile Applications, CHIMIA, 76, 60, https://doi.org/10.2533/chimia.2022.60, 2022.

Kim, M. J., Zoerb, M. C., Campbell, N. R., Zimmermann, K. J., Blomquist, B. W., Huebert, B. J., and Bertram, T. H.: Revisiting benzene cluster cations for the chemical ionization of dimethyl sulfide and select volatile organic compounds, Atmospheric Meas. Tech., 9, 1473–1484, https://doi.org/10.5194/amt-9-1473-2016, 2016.

Kleffmann, J.: Daytime Sources of Nitrous Acid (HONO) in the Atmospheric Boundary Layer, ChemPhysChem, 8, 1137–1144, https://doi.org/10.1002/cphc.200700016, 2007.

Klepeis, N. E., Gabel, E. B., Ott, W. R., and Switzer, P.: Outdoor air pollution in close proximity to a continuous point source, Atmos. Environ., 43, 3155–3167, https://doi.org/10.1016/j.atmosenv.2009.03.056, 2009.

Krechmer, J., Lopez-Hilfiker, F., Koss, A., Hutterli, M., Stoermer, C., Deming, B., Kimmel, J., Warneke, C., Holzinger, R., Jayne, J., Worsnop, D., Fuhrer, K., Gonin, M., and de Gouw, J.: Evaluation of a New Reagent-Ion Source and Focusing Ion–Molecule Reactor for Use in Proton-Transfer-Reaction Mass Spectrometry, Anal. Chem., 90, 12011–12018, https://doi.org/10.1021/acs.analchem.8b02641, 2018.

Krilaviciute, A., Heiss, J. A., Leja, M., Kupcinskas, J., Haick, H., and Brenner, H.: Detection of cancer through exhaled breath: a systematic review, Oncotarget, 6, 38643–38657, https://doi.org/10.18632/oncotarget.5938, 2015.

Lee, B. H., Lopez-Hilfiker, F. D., Mohr, C., Kurtén, T., Worsnop, D. R., and Thornton, J. A.: An Iodide-Adduct High-Resolution Time-of-Flight Chemical-Ionization Mass Spectrometer: Application to Atmospheric Inorganic and Organic Compounds, Environ. Sci. Technol., 48, 6309–6317, https://doi.org/10.1021/es500362a, 2014.

Li, X.-B., Zhang, C., Liu, A., Yuan, B., Yang, H., Liu, C., Wang, S., Huangfu, Y., Qi, J., Liu, Z., He, X., Song, X., Chen, Y., Peng, Y., Zhang, X., Zheng, E., Yang, L., Yang, Q., Qin, G., Zhou, J., and Shao, M.: Assessment of long tubing in measuring atmospheric trace gases: applications on tall towers, Environ. Sci. Atmospheres, 3, 506–520, https://doi.org/10.1039/D2EA00110A, 2023.

Murschell, T., Fulgham, S. R., and Farmer, D. K.: Gas-phase pesticide measurement using iodide ionization time-of-flight mass spectrometry, Atmospheric Meas. Tech., 10, 2117–2127, https://doi.org/10.5194/amt-10-2117-2017, 2017.

Puttu, U., Kamp, J. R., Chen, X., Chen, J.-H., Wang, B., Li, J., Gonzalez-Meler, M. A., Wang, J., and Xu, L.: Chemical ionization mass spectrometry utilizing benzene cations for measurements of volatile organic compounds and nitric oxide, Atmospheric Meas. Tech., 19, 1421–1439, https://doi.org/10.5194/amt-19-1421-2026, 2026.

Riva, M., Pospisilova, V., Frege, C., Perrier, S., Bansal, P., Jorga, S., Sturm, P., Thornton, J. A., Rohner, U., and Lopez-Hilfiker, F.: Evaluation of a reduced-pressure chemical ion reactor utilizing adduct ionization for the detection of gaseous organic and inorganic species, Atmospheric Meas. Tech., 17, 5887–5901, https://doi.org/10.5194/amt-17-5887-2024, 2024.

Seigneur, C., Tesche, T. W., Roth, P. M., and Liu, M.-K.: On the treatment of point source emissions in urban air quality modeling, Atmospheric Environ. 1967, 17, 1655–1676, https://doi.org/10.1016/0004-6981(83)90174-9, 1983.

Sethi, S., Nanda, R., and Chakraborty, T.: Clinical Application of Volatile Organic Compound Analysis for Detecting Infectious Diseases, Clin. Microbiol. Rev., 26, 462–475, https://doi.org/10.1128/CMR.00020-13, 2013.

Sörgel, M., Regelin, E., Bozem, H., Diesch, J.-M., Drewnick, F., Fischer, H., Harder, H., Held, A., Hosaynali-Beygi, Z., Martinez, M., and Zetzsch, C.: Quantification of the unknown HONO daytime source and its relation to NO_2, Atmospheric Chem. Phys., 11, 10433–10447, https://doi.org/10.5194/acp-11-10433-2011, 2011.

Tsai, W.-T.: Toxic Volatile Organic Compounds (VOCs) in the Atmospheric Environment: Regulatory Aspects and Monitoring in Japan and Korea, Environments, 3, 23, https://doi.org/10.3390/environments3030023, 2016.

Wallace, L. A.: Personal Exposure To 25 Volatile Organic Compounds Epa's 1987 Team Study in Los Angeles, California, Toxicol. Ind. Health, 7, 203–208, https://doi.org/10.1177/074823379100700523, 1991.

Warneke, C., Veres, P., Holloway, J. S., Stutz, J., Tsai, C., Alvarez, S., Rappenglueck, B., Fehsenfeld, F. C., Graus, M., Gilman, J. B., and De Gouw, J. A.: Airborne formaldehyde measurements using PTR-MS: calibration, humidity dependence, inter-comparison and initial results, Atmospheric Meas. Tech., 4, 2345–2358, https://doi.org/10.5194/amt-4-2345-2011, 2011.

Yeoman, A. M., Shaw, M., Carslaw, N., Murrells, T., Passant, N., and Lewis, A. C.: Simplified speciation and atmospheric volatile organic compound emission rates from non-aerosol personal care products, Indoor Air, 30, 459–472, https://doi.org/10.1111/ina.12652, 2020.